Nonlinear Cavity and Frequency Comb Radiations Induced by Negative Frequency Field Effects

Cristian Redondo Lourés, Daniele Faccio, and Fabio Biancalana
School of Engineering and Physical Sciences, Heriot-Watt University, EH14 4AS Edinburgh, United Kingdom
(Received 9 June 2015; published 6 November 2015)

Optical Kerr frequency combs (KFCs) are an increasingly important optical metrology tool with applications ranging from ultraprecise spectroscopy to time keeping. KFCs may be generated in compact resonators with extremely high quality factors. Here, we show that the same features that lead to high quality frequency combs in these resonators also lead to an enhancement of nonlinear emissions that may be identified as originating from the presence of a negative frequency (NF) component in the optical spectrum. While the negative frequency component of the spectrum is naturally always present in the real-valued optical field, it is not included in the principal theoretical model used to model nonlinear cavities, i.e., the Lugiato-Lefever equation. We therefore extend these equations in order to include the contribution of NF components and show that the predicted emissions may be studied analytically, in excellent agreement with full numerical simulations. These results are of importance for a variety of fields, such as Bose-Einstein condensates, mode-locked lasers, nonlinear plasmonics, and polaritonics.

DOI: 10.1103/PhysRevLett.115.193904 PACS numbers: 42.65.Sf, 42.60.Da, 42.65.Tg

Introduction.—Kerr frequency combs (KFCs), i.e., light sources with a large number of highly resolved and nearly equidistant spectral lines, have been attracting a considerable interest in recent years, due to their important applications in metrology, optical clocks, precision spectroscopy, precision time and distance measurements, and attosecond pulse generation, to name just a few applications [1–3]. Physical systems that are able to generate KFCs are microring resonators, microtoroids, crystalline resonators, microspheres, photonic-crystal cavities, and optical fiber loops [1]. Microring resonators are particularly important in this respect, since they are small-size, low-loss, CMOS-compatible and power efficient devices that can be made of different nonlinear materials and are therefore ideal for on-chip KFC generation.

The main ingredients for efficient KFC formation have been identified to be four-wave mixing and temporal cavity soliton (CS) generation [2]. There is currently intense research activity aiming to maximize the spectral extent of the comb and its coherence, and to understand the experimentally obtained spectra from first principles. Because of the extremely complex dynamical behavior and stability properties of the propagating CSs and patterns in the resonators, intense theoretical activity related to the mathematical properties of the traditionally used averaged propagation equation, called the temporal Lugiato-Lefever equation (LLE), has developed over the past years, with a frequent display of new and surprising results [3–7].

One of the major dynamical effects in the propagation of ultrashort pulses is the radiation emitted by solitons due to higher-order dispersion effects, also called resonant radiation (RR) [8–11]. This radiation, which appears when pumping near the zero-dispersion point of the structure, is very visible in experiments performed with optical fibers and it also plays a central role in the dynamics of CSs [6,12–14]. Indeed, it has been shown experimentally that CSs emit RR in microring resonators and fiber loops [14–16].

In this Letter we show how negative frequency (NF) effects [17,18] are enhanced in optical microcavities and lead to significant emissions in optical KFCs. We expect the signatures of this process to be already present in existing experimental data, and that future experiments will be able to clearly identify these effects, thus providing an additional tool for the investigation of the fundamental properties of light propagation. In order to do this, we extend the temporal LLE in order to take into account the effects of negative frequencies and conjugate fields on the propagation of CSs in optical resonators (extended LLE, or eLLE for brevity). We show that due to the forced and dissipative nature of the eLLE, the new resonant radiations, which are typically remarkably feeble in conventional optical fibers and bulk materials, can become quite strong and can be more efficiently generated. This surprising result has the potential to impact considerably the formation of KFCs due to CSs and also the intrinsic stability of the homogeneous steady state continuous wave (cw) solutions of the cavity.

Extended temporal Lugiato-Lefever equation—The starting point of any discussion on optical resonators and cavities is the infinite-dimensional Ikeda map [19,20]

$$A_{n+1}(0,t) = TA_{\mathrm{in}}(t) + Re^{-i\phi_0}A_n(L,t), \tag{1}$$

$$i\partial_z A_n + i\frac{\alpha_i}{2}A_n + \hat{D}(i\partial_t)A_n + \hat{S}(i\partial_t)p_{\mathrm{nl}}[A_n] = 0. \tag{2}$$

Here, $A_{\rm in}$ is the envelope of the (impulsed or cw) pump field, T is the transmission coefficient at the coupling point $z=0$, R is the reflection coefficient ($R^2+T^2=1$), $\phi_0=\delta_0-2\pi m$ is the phase accumulated over a round-trip, δ_0 is the cavity detuning, L is the length of the cavity, $A_n(z,t)$ is the envelope of the intracavity field circulating at the nth step, z is the spatial coordinate along the cavity, t is the "fast" time variable in the reference frame moving at the group velocity $1/\beta_1$, $\hat{D}(i\partial_t)\equiv\sum_{j\geq 2}\beta_j(i\partial_t)^j/j!$ is the dispersion operator, $\beta_j\equiv[\partial_\omega^j\beta(\omega)]_{\omega=\omega_0}$ is the jth dispersion coefficient calculated at the pump frequency ω_0, and $\hat{S}(i\partial_t)\equiv(1+i\omega_0^{-1}\partial_t)$ is the shock operator describing the first order correction due to the frequency dependent nonlinearity.

The Ikeda map of Eqs. (1) and (2) is usually based on the slowly varying envelope approximation (SVEA), under which the spectral extent of the pulse must be much smaller than its central frequency. In Eq. (2), $p_{\rm nl}$ is the nonlinear polarization of the intracavity field, which in the presence of the Kerr effect alone can be written as $p_{\rm nl}[A_n]=\gamma|A_n|^2A_n$, where γ is the nonlinear coefficient of the material. However, in order to include in a physically consistent way the higher-order effects such as third-harmonic generation (THG) and the contribution of conjugate terms, one can use the so-called analytic signal representation for all the fields involved in Eqs. (1) and (2). This formulation completely avoids the use of the SVEA in the equations, conserves energy even in presence of THG, and can treat pulses of arbitrary durations. In such a way, the contribution of the negative frequency components of the pulse are fully taken into account, and this allows us to describe the nonlinear dynamics of the full-field nonlinear forward Maxwell equations. We refer the reader to Refs. [18,21,22] for an in-depth discussion.

The analytic signal of the nonlinear polarization is written as [18,21,22]

$$p_{\rm nl}[A_n]=\gamma\left[|A_n|^2A_n+|A_n|^2A_n^*e^{2i\phi(z,t)}+\frac{1}{3}A_n^3e^{-2i\phi(z,t)}\right]_+, \tag{3}$$

where $\phi(z,t)\equiv\omega_0 t+\Delta k z$, and $\Delta k\equiv(\beta_1\omega_0-\beta_0)$ is a factor, crucial for the efficient phase matching of the resonant negative-frequency terms, that measures the difference between the phase and the group velocity in the medium. The subscript $+$ in Eq. (3) signifies the filtering of the negative frequency components out of the polarization. This ensures that during its evolution $A_n(z,t)$ only contains positive frequencies, and it is thus consistent with its own definition. The first term in Eq. (3) is the usual Kerr term, the second is the so-called "negative Kerr" (NK) term, while the third gives THG. Note that the NK and THG terms must appear together in order to preserve the Hamiltonian nature of the four-wave mixing interaction, something that was overlooked prior to our theoretical work on the subject [18].

Equations (1) and (2) can be made more tractable by now following the same Lugiato-Lefever approach [23]. To this aim, we now plug Eq. (3) into Eq. (2), and we follow the averaging procedure described in Ref. [20], using the "cavity soliton units" $\xi\equiv z/L_{D2}$, $\tau\equiv t/t_0$, $\Omega\equiv\omega_0 t_0$, $\kappa\equiv\Delta k L_{D2}$, $\psi\equiv A/\sqrt{P_0}$, and $P_0\equiv(\gamma L_{D2})^{-1}$ (so that $L_{\rm NL}\equiv[\gamma P_0]^{-1}=L_{D2}$), $\psi_{\rm in}\equiv A_{\rm in}/\sqrt{P_0}$, and $\phi(\xi,\tau)\equiv\Omega\tau+\kappa\xi$. A natural value for the time scale t_0 is the typical single-CS duration $t_0=[|\beta_2|L/(2\delta_0)]^{1/2}$. In the averaging procedure, the cavity length L must be much smaller than the dispersive and nonlinear lengths L_{D2} and $L_{\rm NL}$, respectively. This ensures that the intracavity pulse does not change much during a single round-trip. This slow variation must also be satisfied by the NK and THG terms in Eq. (3): the phase $\phi(z,t)$ must rotate very rapidly over a single round-trip, so that the average effect is mediated almost to zero, resulting in the condition $\kappa\gg 1$.

In this way, we arrive at the following eLLE:

$$i\partial_\xi\psi+\hat{D}(i\partial_\tau)\psi+i(\Gamma+i\delta)\psi+(1+i\Omega^{-1}\partial_\tau)\times\left[|\psi|^2\psi+|\psi|^2\psi^*e^{2i\phi(\xi,\tau)}+\frac{1}{3}\psi^3e^{-2i\phi(\xi,\tau)}\right]_+-i\mu\psi_{\rm in}=0. \tag{4}$$

$\Gamma\equiv[(\alpha_{\rm i}L+T^2)/2]L_{D2}/L$, $\delta\equiv\delta_0L_{D2}/L$, $\mu\equiv TL_{D2}/L$, $\hat{D}(i\partial_\tau)\equiv\sum_{n\geq 2}b_n(i\partial_\tau)^n$, where $b_n\equiv\beta_n/(n!t_0^{n-2}|\beta_2|)$ are the dimensionless dispersion coefficients, and $\phi(\xi,\tau)\equiv\Omega\tau+\kappa\xi$.

Equation (4) is the central result of this Letter. It can be applied to any kind of optical resonator, and can be easily extended to include the Raman effect or any other perturbation of the nonlinear Schrödinger equation (NLS).

Phase matching conditions for the new radiations.—We now derive the phase-matching conditions for the most important resonant radiations emitted by the ultrashort CSs propagating in the resonator. In Eq. (4), we substitute the ansatz $\psi(\tau,t)=\psi_0+g(\xi,\tau)$, and linearize with respect to the small radiation field g. Note that due to the loss term proportional to Γ in Eq. (4), far from the central peak of the CS the resonant radiations decay asymptotically towards the complex cw background ψ_0. We use the perturbation method employed in Ref. [18] in the fiber-optics or bulk context, obtaining

$$D(\Delta)-v\Delta=D_0, \tag{5}$$

$$D(\Delta)-v\Delta=D_0\pm 2\kappa, \tag{6}$$

where Δ is the dimensionless frequency detuning from the pump, $D(\Delta)\equiv\sum_{n\geq 2}b_n\Delta^n$ is the dispersion of the linear waves, $D_0\equiv\delta-i\Gamma-2|\psi_0|^2$ is the complex nonlinear wave number, and v is the velocity parameter of the

resulting moving CS, which starts to drift as a consequence of the higher-order dispersion [12]. Equation (5) is connected to the emission of the conventional RR, routinely observed in fibers and cavities [10,11,14]. Equations (6) phase match the negative frequency resonant radiation [NRR, "+" sign in Eq. (6)], which is due to the NK term in Eq. (3), and the third-harmonic resonant radiation [THRR, "−" sign in Eq. (6)], which is due to the THG term in Eq. (3). Note that in all physically relevant situations $\kappa \gg |D_0|, |v\Delta|$. The roots of Eqs. (5) and (6) have real and imaginary parts, indicating the frequency detuning of the emissions and their decay rate towards the soliton background, respectively. Equation (5) is valid only in the presence of propagating CSs, while Eqs. (6) holds also for a pure cw intracavity field. This latter phase-matching equation implies that the usual stable branch of the stationary solutions of Eq. (4), i.e., the smallest root of the equation $i(\Gamma + i\delta)\psi + |\psi|^2\psi - i\mu\psi_{\rm in} = 0$ (see also Refs. [24,25]), is unstable in the presence of the NK and THG terms, and sidebands will appear. These emissions, which are not present in the traditional temporal LLE, are a new feature of our eLLE model.

Numerical simulations.—We illustrate the spectral dynamics and the emission of the resonant radiations from ultrashort CSs as seen in the previous section by using a highly nonlinear, small, low-loss resonator (e.g., a microtoroid or a microring, similar to those described in Refs. [1,2], see also Fig. 1). We take a radius $r = 30\,\mu$m, cavity length $L = 1.88 \times 10^{-4}$ m, pump wavelength $\lambda_0 = 1.55\,\mu$m, $\beta_2 = -90$ ps^2/km, $\beta_3 = -1.11$ ps^3/km, nonlinear coefficient $\gamma = 1$ W^{-1} m^{-1}, group index at the pump $n_g = 1.5$, cw pump power $P_{\rm in} = 265$ mW, transmission coefficient $T = 0.07$, detuning from the cavity resonance $\delta_0 = 0.0115 \ll \pi$, free spectral range FSR = 1060 GHz, round-trip time $t_R = 1/\text{FSR} = 150$ fs, photon lifetime $t_{\rm ph} \simeq 0.19$ ns, finesse $\mathcal{F} \simeq 628$, and loaded Q factor

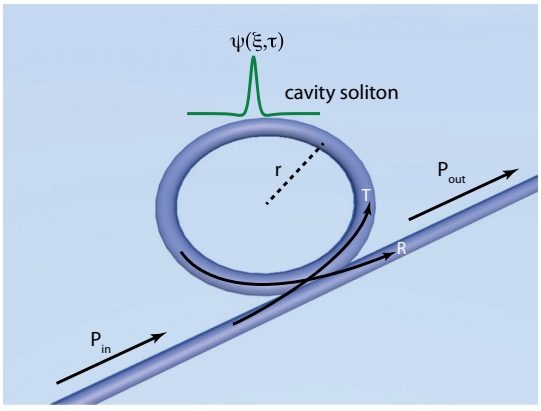

FIG. 1 (color online). Sketch of the generic microcavity and its parameters. r is the ring radius, $P_{\rm in}$ is the cw input power, $P_{\rm out}$ is the output field power, $\psi(\xi,\tau)$ is the intracavity field at position ξ in the ring, and R and T are the reflection and transmission coefficients, respectively.

$Q \sim 10^5$. The typical temporal width of the CSs formed in the cavity is $t_0 = [|\beta_2|L/(2\delta_0)]^{1/2} \simeq 27$ fs, and we take this value for the scaling of Eq. (4). The typical peak power of the CS is also given by the soliton power scale $P_0 = 2\delta_0(L_{D2}/L) = [\gamma L_{D2}]^{-1} \simeq 122$ W. The second order dispersion length is $L_{D2} = 8.2$ mm, which gives a ratio $L_{D2}/L \simeq 43.5 \gg 1$, making the averaging procedure meaningful. We take $\Delta k \sim 0.67 \times 10^4$ m^{-1}, an order of magnitude that is common for solid media. With these parameters, the dimensionless coefficients in Eq. (4) become $\Gamma = 0.217$, $\delta = 0.5$, $\mu = 3$, $\psi_{\rm in} = 0.047$, $b_2 = \pm 0.5$, $b_3 = -0.0758$, $\Omega = 33$, and $\kappa \simeq 54.5$.

Figure 2(a) shows the output spectrum of the propagation ($\xi = 27$, equivalent to 1200 cavity round-trips) of the lower-branch homogeneous steady state (HSS) cw solution (see Refs. [24,25]) in both anomalous and normal dispersions, respectively ($b_2 = \pm 0.5$), by using the eLLE (4), when $b_3 = 0$. As discussed in the previous section, for these parameters the HSS solution is stable in the absence of the NK and THG terms. Conversely, accounting for the complex conjugate fields leads to far-detuned sidebands (indicated by $P1$ and $P2$ in the figure) according to the phase-matching conditions of Eq. (6), which grow very quickly after four to five round-trips ($\xi \simeq 0.1$, i.e., $\sim 80\,\mu$m) and then perfectly stabilize. Note that these new emissions appear irrespective of the sign of b_2, due to the $\pm$ sign in Eq. (6). Moreover, the sidebands would be perfectly symmetric with respect to the pump frequency for vanishing higher-order dispersion terms, but become asymmetric when the contribution of $b_{n\geq 3}$ is important, see Fig. 2(b), showing that this process is not due to conventional Kerr four-wave mixing. In this case, the two peaks are always slightly unbalanced in amplitude due to the presence of

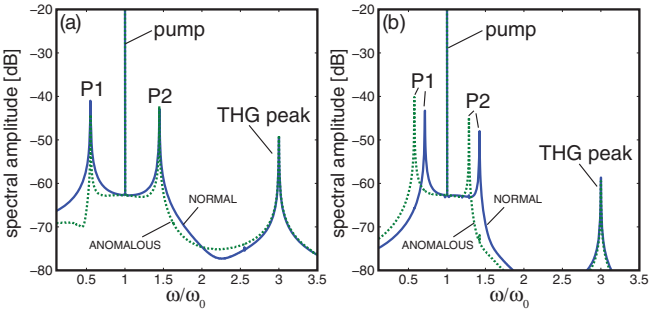

FIG. 2 (color online). (a) Output spectrum of the propagation of the HSS cw solution for normal ($b_2 = +0.5$, blue solid line) and anomalous ($b_2 = -0.5$, green dashed line) dispersions, in the case $b_3 = 0$. The propagation distance is $\xi = 27$. (b) Same as (a) but with $b_3 = -0.0758$. All other relevant parameters are given in the text. The pump maximum, located at 0 dB, is cut for clarity. As an example, in (b), the positions of $P1$ and $P2$ are (in units of ω/ω_0) 0.5759 and 1.2859 for anomalous dispersion and 0.7141 and 1.4241 for normal dispersion. Equations (5) and (6) predict 0.5756 and 1.2862 for the former case and 0.7123 and 1.4241 for the latter, showing excellent agreement.

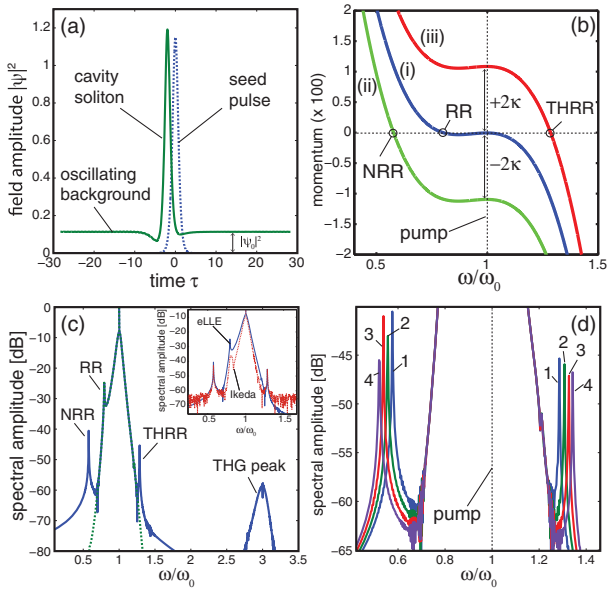

FIG. 3 (color online). (a) Formation of a stable moving CS in the cavity, after a propagation of $\xi = 27$. (b) Real part of phase-matching curves for the three equations (5) and (6): (i) for Eq. (5), (ii) for Eq. (6) with the + sign, and (iii) for Eq. (6) with the − sign. Circles are the predicted positions of all the generated radiations (RR, NRR, THRR). (c) Intracavity field spectrum at $\xi = 27$, when considering only the Kerr term (green dashed line), and when including the NK and the THG terms in Eq. (3) (blue solid line). The resonant radiations generated by the NK and the THG terms are indicated with NRR and THRR, respectively. Inset: comparison between the Ikeda map of Eqs. (1) and (2) and the eLLE (4) for $\xi = 27$. (d) Enlargement of the NRR and THRR peaks when $\kappa = 54.5$, 65, 76, 87 (indicated by 1, 2, 3, 4, respectively). The parameters of the simulation can be found in the text, and $b_2 = -0.5$, $b_3 = -0.0758$, $v = 0.084$.

THG and pump and loss in the system. This proves, for the first time to our knowledge, the existence of novel kinds of emissions in the cw regime that are due to the contribution of negative frequencies in the nonlinear polarization [Eq. (3)].

Figure 3(a) shows the formation of a stable moving CS in the cavity, in the presence of third-order dispersion, $b_3 \neq 0$, and in anomalous dispersion, $b_2 = -0.5$, when using the eLLE (4). The input seed is taken to be $\psi(\xi = 0, \tau) = \sqrt{2\delta}\,\mathrm{sech}(\sqrt{2\delta}\tau)$, i.e., the autosolution of the pulsed cavity [25], which is a good approximation (albeit with vanishing background) of the final CS. Figure 3(b) shows the real part of the phase-matching curves of Eqs. (5) and (6), and the prediction of the frequency positions of all the resonant radiations. The green dashed line in Fig. 3(c) shows the intracavity field spectrum, in the case when only the Kerr effect is present in the nonlinear polarization of Eq. (3) (i.e., the case of the conventional temporal LLE). In this case, only the usual RR peak, which satisfies Eq. (5), is emitted near the pump (with a very small contribution from its symmetric counterpart, not discussed here, see Ref. [12]).

The solid blue line in Fig. 3(c) shows the spectrum when taking into account all the terms in the full polarization, which contains also the NK and the THG terms, see Eq. (3). One can notice the appearance of relatively strong peaks, which are the NRR and the THRR peaks described in the previous section. Equations (5) and (6) predict peaks located at $\omega/\omega_0 = 1.286247$ (THRR), 0.575641 (NRR), 0.79236 (RR), while the simulation based on Eq. (4) [Fig. 3(c)] shows peaks at $\omega/\omega_0 = 1.286$, 0.5759, and 0.7926, showing excellent agreement between theory and simulations. The inset in Fig. 3(c) also shows the comparison between the results of Eq. (4) and the Ikeda map of Eqs. (1) and (2). For these parameters, excellent qualitative agreement is found. Figure 3(d) shows the position of the NRR and THRR peaks for different values of κ. The amplitudes of the radiations vary since the CS background oscillates during propagation.

Discussion and conclusions.—Our results show that frequency comb formation in Kerr media is affected by the resonant radiations resulting from the nonlinear interactions between positive and negative frequencies. These new types of emissions play a conceptually important but somewhat minor role in optical fibers and bulk materials. However, in optical resonators such as fiber loops and microrings, the field is forced to circulate many times in the cavity, and CSs possess a cw background that may dramatically enhance the emission of the new radiations. As a consequence, the output KFC spectra are affected by the radiation peaks emitted by CSs and the "negative frequency" radiations play an important role. We have provided the derivation of a universal model (the eLLE), not based on the SVEA, that is able to take into account the full dynamics of the ultrashort intracavity pulses, and is amenable to analytical investigations. Because the universality of the NLS-type equations, our results can open new opportunities in very diverse fields, such as Bose-Einstein condensates, mode-locked fiber lasers, nonlinear plasmonics, and cavity polaritonics. The contribution of the conjugate fields, which leads to the nonlinear interaction between the positive and negative frequency components, is usually neglected in many areas of physics, but it can have profound consequences for their nonlinear dynamics.

D. F. acknowledges financial support from the European Research Council under the European Union's Seventh Framework Programme (FP/2007–2013)/ERC GA 306559 and EPSRC (UK, Grant No. EP/J00443X/1).

[1] T. J. Kippenberg, R. Holzwarth, and S. A. Diddams, Science **332**, 555 (2011).
[2] T. Herr, V. Brasch, J. D. Jost, C. Y. Wang, N. M. Kondratiev, M. L. Gorodetsky, and T. J. Kippenberg, Nat. Photonics **8**, 145 (2013).
[3] V. E. Lobanov, G. Lihachev, T. J. Kippenberg, and M. L. Gorodetsky, Opt. Express **23**, 7713 (2015).

[4] P. Parra-Rivas, D. Gomila, M. A. Matías, P. Colet, and L. Gelens, Opt. Express **22**, 30943 (2014).
[5] P. Parra-Rivas, D. Gomila, M. A. Matias, S. Coen, and L. Gelens, Phys. Rev. A **89**, 043813 (2014).
[6] P. Parra-Rivas, D. Gomila, F. Leo, S. Coen, and L. Gelens, Opt. Lett. **39**, 2971 (2014).
[7] A. Coillet, J. Dudley, G. Genty, L. Larger, and Y. K. Chembo, Phys. Rev. A **89**, 013835 (2014).
[8] N. Akhmediev and M. Karlsson, Phys. Rev. A **51**, 2602 (1995).
[9] A. V. Husakou and J. Herrmann, Phys. Rev. Lett. **87**, 203901 (2001).
[10] F. Biancalana, D. V. Skryabin, and A. V. Yulin, Phys. Rev. E **70**, 016615 (2004).
[11] D. V. Skryabin, F. Luan, J. C. Knight, and P. St. J. Russell, Science **301**, 1705 (2003).
[12] C. Millián and D. V. Skryabin, Opt. Express **22**, 3732 (2014).
[13] S. Coen, H. G. Randle, T. Sylvestre, and M. Erkintalo, Opt. Lett. **38**, 37 (2013).
[14] J. K. Jang, M. Erkintalo, S. G. Murdoch, and S. Coen, Opt. Lett. **39**, 5503 (2014).
[15] M. R. E. Lamont, Y. Okawachi, and A. L. Gaeta, Opt. Lett. **38**, 3478 (2013).
[16] Y. Okawachi, K. Saha, J. S. Levy, Y. Henry Wen, M. Lipson, and A. L. Gaeta, Opt. Lett. **36**, 3398 (2011).
[17] E. Rubino, J. McLenaghan, S. C. Kehr, F. Belgiorno, D. Townsend, S. Rohr, C. E. Kuklewicz, U. Leonhardt, F. König, and D. Faccio, Phys. Rev. Lett. **108**, 253901 (2012).
[18] M. Conforti, A. Marini, T. X. Tran, D. Faccio, and F. Biancalana, Opt. Express **21**, 31239 (2013).
[19] M. Haelterman, S. Trillo, and S. Wabnitz, Opt. Commun. **91**, 401 (1992).
[20] M. Haelterman, S. Trillo, and S. Wabnitz, Opt. Lett. **17**, 745 (1992).
[21] Sh. Amiranashvili, U. Bandelow, and N. Akhmediev, Phys. Rev. A **87**, 013805 (2013).
[22] Sh. Amiranashvili and A. Demircan, Adv. Opt. Technol. **2011**, 989515 (2011).
[23] L. A. Lugiato and R. Lefever, Phys. Rev. Lett. **58**, 2209 (1987).
[24] I. V. Barashenkov and Yu. S. Smirnov, Phys. Rev. E **54**, 5707 (1996).
[25] S. Coen and M. Erkintalo, Opt. Lett. **38**, 1790 (2013).